CHAPTER VI
INFLUENCE OF POTASSIUM LOADING AND CALCINATION TEMPERATURE ON THE ACTIVITY OF KOH/MORDENITE ZEOLITE FOR TRANSESTERIFICATION OF PALM OIL

6.1 Abstract

A series of K/mordenite with different potassium loading have been studied as a heterogeneous catalyst for transesterification of palm oil using a batch reactor and a packed-bed reactor. The 20 %K/mordenite processed in a batch reactor gave the highest methyl ester yield of 96.67 % under optimum condition, while the methyl ester over 94 % was obtained in a packed-bed reactor. The prepared catalysts were characterized by using XRD, XRF, N_2 adsorption-desorption, Hammett indicators, acid titration, and SEM. Dealumination was found under calcined catalysts at a high temperature and had a significant effect on the physical structure and chemical composition of the catalysts. Leaching of potassium species was negligible, whereas depositing and washing of the reacted mixture with acetone on the catalyst surface were observed by FTIR. The packed-bed reactor exhibited higher possibility to regenerate catalyst than the batch reactor.

6.2 Introduction

Biodiesel, as an alternative fuel, has the potential to contribute toward sustainable development of many countries. The main advantages of using biodiesel as a fuel are its renewability, biodegradability and more eco-friendly emission exhaust gases [1]. Biodiesel can normally be used not only as a fuel in a diesel engine but also for lubricity, which leads to decreased injector coking and trumpet formation on the injectors, and less carbon deposits in an engine [2,3]. Compared to fossil fuel, biodiesel has lower emissions of unburned hydrocarbons, particulate matter, and air toxins when operated in a diesel engine.

Industrial biodiesel, generally produced by a chemical reaction between vegetable oils or animal fats, and alcohol—such as methanol or ethanol—is known

as transesterification. To accelerate this reaction, a catalyst is required usually a strong base, such as NaOH or KOH, is used to produce biodiesel [4]. In general, the main drawbacks of homogeneous base catalysts are the large amount of waste water from the washing step and high energy consumption for phase separation. These problems can be solved with the use of heterogeneous transesterification catalysts, which offer many advantages such as prevention of side reactions and possible reuse of the catalyst. A variety of solid catalysts—such as alkaline and alkaline earth metal oxides, various types of alkali metal compounds supported on alumina—have been examined for this reaction [5–7]. They observed that higher amounts of alkaline result in higher basic properties, which promoted transesterification reaction. However, leaching of K into solution during the course of a reaction has been reported by Alonso *et al.* (2007) and Noiroj *et al.* (2009) [8,9]. Leaching affects the industrial application; moreover, extensive leaching may threaten the reusability of catalyst.

Zeolites, as catalysts and adsorbents, are famous for chemical industry owing to their high surface areas, microporous structures and ability to exchange cationic sites. Zeolite X, mordenite, beta, and NaX zeolites show high efficiencies in biodiesel yield [10,11]. Mordenite has been explored as a support and as a catalyst for many reactions and the modification of alkaline on the zeolite to enhance the electron density of the framework oxygen and to promote the strength of molecular centers has been well documented in the literature. Accordingly, the transesterification of palm oil using alkali loaded on mordenite achieved a high conversion yield, making it of interest to apply in biodiesel production.

Much research has been conducted to investigate the effects of heterogeneous base catalysts in a batch reactor; however, it was found that the stability of the catalyst decreased slightly within the recycle run [12]. Ni and Meunier (2007) proposed the possibility of using fixed-bed reactor systems for the separation of catalyst and product, and increased mechanical stability of the catalyst; therefore, packed-bed reactor was used to resolve these problems [13].

In the present study, the catalytic performances of KOH/mordenite in transesterification under mild condition were determined in both batch and packed-bed reactors to evaluate the suitability of this catalyst. The influence of basic

properties and the physical structure on the catalytic activity were also evaluated. Additionally, the deactivation and the regeneration of catalysts were also investigated.

6.3 Experimental

6.3.1 Batch Reactor

One hundred grams of refined palm oil were placed in a 500 ml three-necked flask. The vegetable oil was heated to 65 °C. Then the catalyst and methanol were added to a three-necked flask. A magnetic stirrer was used for mixing the oil, methanol, and catalyst at 300 rpm. The reaction was carried out until it reached the desired reaction time. The products were analyzed by gas chromatography.

6.3.2 Packed-bed Reactor

Refined palm oil and methanol were weighed and placed into a three-necked flask and heated to 60 °C. The mixture was stirred until it reached the desired temperature and was driven by a peristaltic pump at a rate of 11 ml/min (a residence time W/F = 0.013 g cat/(g feed.h)) to the bottom of the packed-bed reactor. The mixtures were circulated back to the system until they reached the desired reaction time. The products were pumped back into the flask to separate and purify as described in the batch reactor procedure.

6.4 Results and Discussion

6.4.1 Influence of KOH Loading

The XRD patterns of the mordenite and KOH/mordenite catalysts are illustrated in Figure 6.1(a–e). The typical peaks of mordenite at 2θ = 13.5°, 19.6°, 22.3°, 25.7°, 26.3°, 27.5°, and 30.9° are observed. When the loading amount of K was increased, the XRD patterns of the 10 wt%, 15 wt%, and 20 wt% K showed that the intensity of mordenite peaks decreased when the loading amount of K was increased, indicating that a small loss of crystallinity is occurring. However, the K_2O was not observed on the XRD patterns of KOH/mordenite, suggesting that either the intensity

of the K_2O peak was very low compared to the XRD patterns of mordenite zeolite or the significant overlap of its reflections with those of the mordenite. In addition, at high loading amounts of K (30 wt%), the XRD patterns of the prepared catalysts showed an increase in amorphous part.

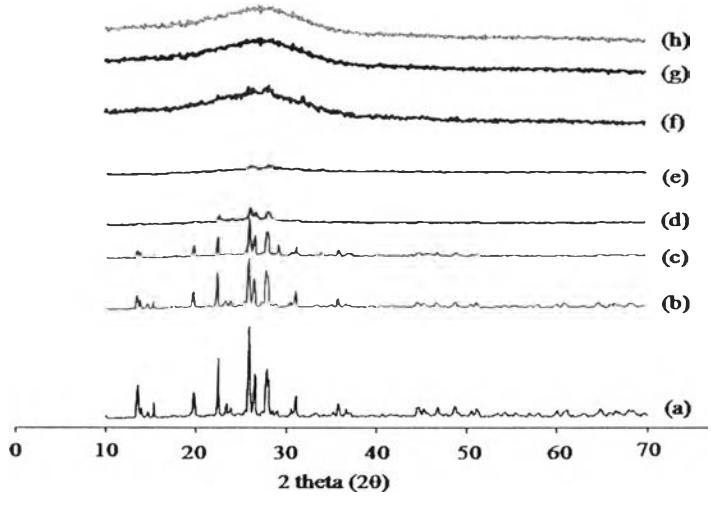

Figure 6.1 XRD patterns of mordenite and K/mordenite catalysts: (a) mordenite, (b) 10 wt% K/mordenite, (c) 15 wt% K/mordenite, (d) 20 wt% K/mordenite, (e) 30 wt% K/mordenite, and calcined 20 wt% K/mordenite at temperature: (f) 400 °C, (g) 500 °C, and (h) 600 °C.

The Si/Al ratio of mordenite in this study was 9.46 (Table 6.1), which is close to Macedonia *et al.* (2000) [14]. The KOH/mordenite catalyst decrease its Si/Al ratio upon treatment (from 9.46 to 9.13), suggesting that Si has been slightly extracted out of the mordenite. Our results corresponded with Guisnet *et al.* (1990) who noted that the decrease in crystallinity was probably due to the absence of extraframework aluminium on the zeolite which could be replaced the silicon [15].

Table 6.1 Characterization of N_2 adsorption and desorption, basic properties and XRF of mordenite and K/mordenite catalyst

Sample	Surface area (m^2/g)	Si/Al Ratio[A]	Basic strength (H_-)[B]	Basicity (mmol/g)			Methyl ester yield (%)		K Leaching (wt% of KOH in palm oil)[A]	
				CO_2-TPD		Estimated titration	C	D	C	D
				110°C	310°C					
Fresh mordenite	315.5	9.46	$H_- < 7.2$	0.049	0.014	0.18	0	0	-	-
Fresh 10 wt% K/mordenite	170.28	-	$9.8 > H_- > 15$	0.022	0.01	2.41	89	-	-	-
Fresh 20 wt% K/mordenite	92.86	9.44	$9.8 > H_- > 15$	0.0037	0.003	5.16	96.67	94.54	-	-
Fresh 30 wt% K/mordenite	1.4	9.13	$9.8 > H_- > 15$	0	0	4.23	70.11	-	-	-
20 wt% K/mordenite Calcined at 400 °C	12.7	-	$9.8 > H_- > 15$		-	4.81	82.64	-	-	-
20 wt% K/mordenite Calcined at 500 °C	6.8	11.99	$9.8 > H_- > 15$		-	2.98	38.12	-	-	-
20 wt% K/mordenite Calcined at 600°C	4.5	-	$9.8 > H_- > 15$		-	2.21	18.1	-	-	-
Spent 1st 20 wt% K/mordenite	17.2	9.43	$9.8 > H_- > 15$		-	4.48	72.33	57.71	0.096	0.086
Spent 2nd 20 wt% K/mordenite	-	-	$9.8 > H_- > 15$		-	3.89	40.24	26.08	0.076	-
Treated spent1st 20 wt% K/mordenite	37.8	-	$9.8 > H_- > 15$		-	3.58	-	19.76	-	-
Treated spent2st 20 wt% K/mordenite	-	-	$9.8 > H_- > 15$		-	2.25	-	10.34	-	-

A: Measured by a XRF technique, B: Measured by Hammett indicators, C: Batch reactor, D: Packed-bed reactor

The SEM images revealed that the mordenite and KOH/Mordenite particles irregular in spherical shape with a dimension of 10 μm to 20 μm at a magnification of 1000, as shown in Figure 6.2(a–c). No significant difference in morphology of mordenite and KOH/mordenite was observed. After being loaded with KOH, the prepared catalyst retained its structures; however, the particle size of the catalyst increased with an additional loading amount of K. The morphology of the 30%K/mordenite changed to an amorphous structure due to the damaged structure of the mordenite support. At a magnification of 100k (100 to 500) nm, as shown in Figure 6.2(j–l), the images of mordenite exhibited a round plate shape and sharp crystallinity with the pore diameter averaging 60.8 nm. The pore diameter of mordenite consisted of straight 12-membered right channels with a slightly elliptical cross section of 67 nm x 70 nm [16,17]. When loading K to 20 wt%, the surface of modified mordenite still exhibited a round shape, although crystallinity and pore diameter (~56 nm) were slightly lower than that of the unmodified mordenite. The round plate shape and crystallinity of the mordenite were not found after loading K to 30%. Unfortunately, the excess of potassium at 30 wt% covered all the pores and surface of the zeolite, which resulted in growth of the particle size. This signified how the potassium interacted with the surface of mordenite by SEM, which is consistent with the present XRD results.

The result from N_2 adsorption-desorption (BET method) of the prepared catalyst is shown in Table 6.1. The surface area of the unmodified mordenite decreased from 315.5 m^2/g to 1.4 m^2/g when the potassium content was increased to 30 wt%. The H-K cumulative pore volume curve of pure mordenie and modified mordenite samples are shown in Figure 6.3. The pore volume of mordenite decreased from 0.2516 cm^3/g to 0.0179 cm^3/g, which indicated that the potassium base caused a significant decrease in the pore volume inside a hollow pore. Moreover, the peak width of the curves was analyzed in the range of 3 nm to 400 nm. Microspores were rarely found after increasing the potassium hydroxide to 30 wt% and the pore size distribution of the catalyst decreased which corresponded with the decline in volume of the pores. Simultaneously micropore distribution was narrowed and surface area was greatly reduced at high loading of alkaline solution because of the coverage of potassium which blocked pore openings.

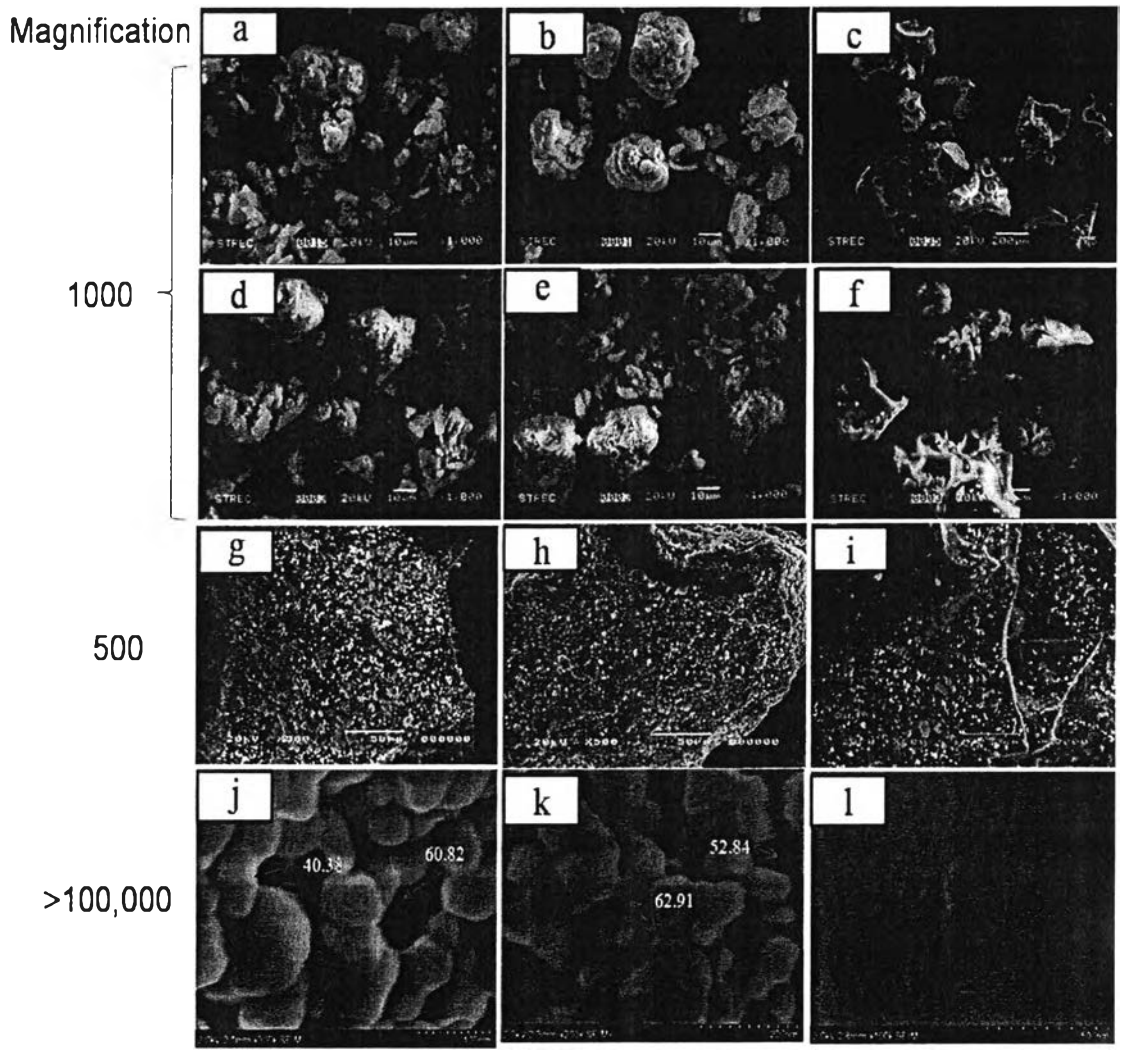

Figure 6.2 SEM patterns of mordenite and K/mordenite catalysts: (a) mordenite, (b) 20 wt% K/mordenite, and (c) 30 wt% K/mordenite: calcined 20 wt% K/Mordenite at temperature: (d) 400 °C, (e) 500 °C, and (f) 600 °C: (g) Fresh 20 wt% K/mordenite, (h) Spent 20 wt% K/mordenite, and (i) Treated 20 wt% K/mordenite: (j) mordenite, (k) 20 wt% K/mordenite, and (l) 30 wt% K/mordenite.

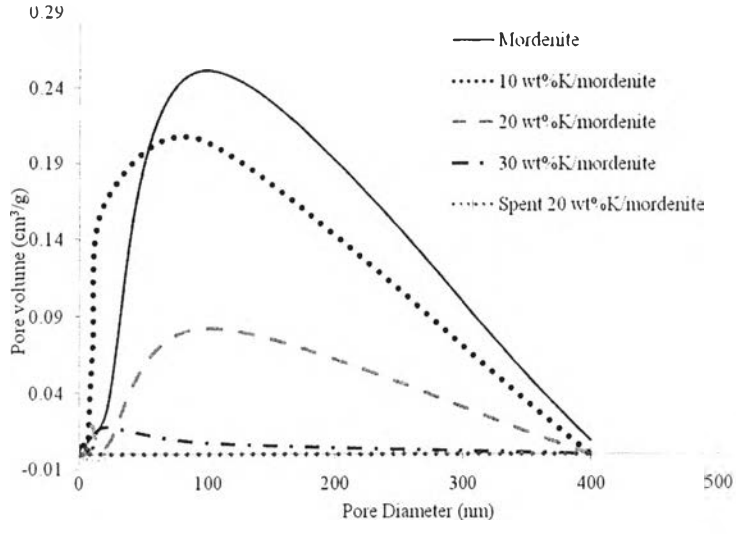

Figure 6.3 Horvath-Kawazoe pore size and pore volume of mordenite and modified mordenite catalysts.

The FTIR spectra of mordenite support and KOH/mordenite catalysts are shown in Figure 6.4. The absorption peaks at 3614 cm^{-1} and 3460 cm^{-1} (Figure 6.4a) were attributed to OH–stretching associated with the terminal silanol groups [18] and the H–O–H frequency of the H_2O molecule was located at a wavenumber of 1629–1646 cm^{-1} at a medium intensity. The set of strong intensity peaks at 1224 cm^{-1} and 1046 cm^{-1} were ascribed to the vibration of external TO4 (T = Al, Si) and the antisymmetrical stretching vibration of the tetrahedral (T–O bonds), respectively. The other groups of absorption band of 628–789 cm^{-1} corresponded to the characteristic vibration of the symmetrical stretching of Si (Al)–O bonds, and the bending of O–Si (Al)–O was interpreted at 437 cm^{-1} [19]. These results confirmed the functional group and the characteristic of the pure mordenite support.

For fresh catalyst (Figure 6.4b), many absorption peaks were transformed due to the loading of K. The reduction of intensity of the OH–stretching vibration at 3600 cm^{-1} changed to a broad band. In addition, the set of high intensity absorption peaks at 1000–1250 cm^{-1} of pure mordenite support converted to a broad peak at 800–1300 cm^{-1} for KOH/mordenite catalysts. It could be inferred that the impregnation of the KOH may have some effects on the structure and composition of

the mordenite zeolite support, which are indications of crystallinity loss, probably as a consequence of dealumination.

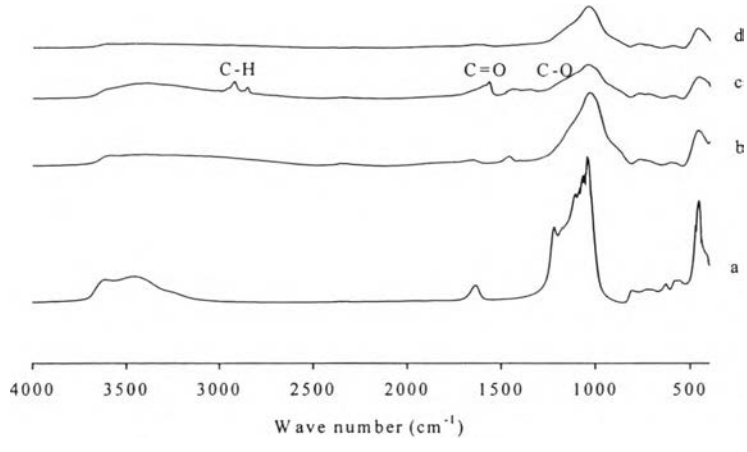

Figure 6.4 FTIR patterns of mordenite and K/mordenite catalysts: (a) mordenite, (b) fresh 20 wt% K/mordenite, (c) used 20 wt% K/mordenite, and (d) washed 20 wt% K/mordenite.

To investigate chemical properties of the catalysts, the basic properties of these catalysts were observed by using CO_2-TPD, as shown in Figure 6.5. The mordenite zeolite was exposed CO_2 at 110 °C and 300 °C where the molecules interacted weakly and then strongly on the surfaces, respectively. It did not show the desorption peak at high temperature, which attributed to the interaction of CO_2 with the occluded sodium oxide species [20]. When potassium loading was increased on the mordenite, a stronger basic site could be observed at the higher temperature; however, desorption peaks were not found until 900 °C. The intensity of the CO_2 desorption peak at low temperature decreased when high amount of potassium content were used. In fact, mordenite did not show any catalytic activity while KOH/mordenite with the highest basicity (from titration method) showed the highest activity. The CO_2 adsorption properties of zeolites are also influenced by the porous characteristics of the framework. This was attributed to the different Si/Al ratios of the zeolites as well as the amount and type of charge-balancing cations.

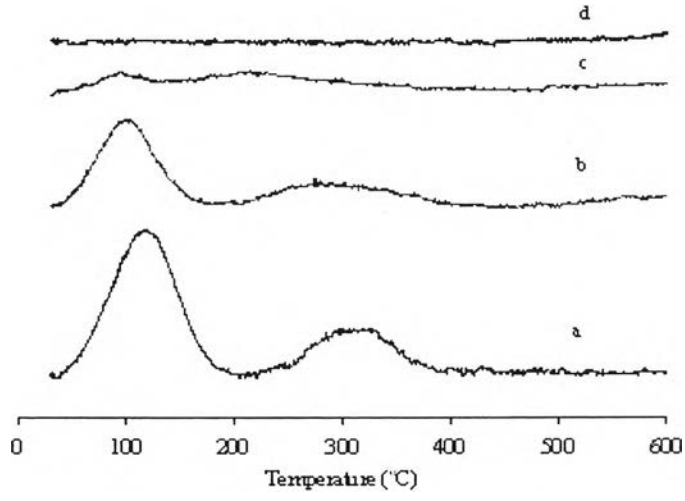

Figure 6.5 CO_2-TPD patterns of mordenite and K/mordenite catalysts: (a) mordenite, (b) 10 wt% K/mordenite, (c) 20 wt% K/mordenite, and (d) 30 wt% K/mordenite.

To clarify the amount of potassium with basic properties, Hammett indicators were used to indicate the basic strength that existed on the surface of the catalyst, as shown in Table 6.1. The pure mordenite zeolite had no basic property and the modified mordenite showed higher basic strength in the range of $9.8 > H_- > 15$ when loading amount of KOH was increased, this resulted in higher conversion rate. However, the basic strength value could not be used to clarify the activity of the prepared catalysts. Thus, the basic site of the catalyst was measured by the approximated acid titration method, as shown in Table 6.1. It was found that the basic sites increased with increased K loading to 20 wt%K. With further increases the K > 20 wt%, the basic sites decreased slightly. Therefore, the highest basic site was obtained at 20 wt% K/mordenite for the uncalcined catalyst. The different amount of basic sites between CO_2-TPD and approximated titration was obviously observed. The CO_2-TPD technique used CO_2 gas as a probe molecule absorbing on the surface catalyst. The molecular size of CO_2 is approximately 37.94 nm [21], which it can diffuse into the micropore of the mordenite zeolite. The chemisorbed CO_2 played an important role in measuring the basic species which were exposed on the surface. The pore structure of mordenite collapsed at 30 wt%K/mordenite, which

was previously explained in XRD, SEM and N_2 adsorption-desorption techniques. The CO_2 gas could not diffuse to absorb on the surface in the pores of the zeolite, thus, basic sites of the catalyst decreased. However, the titration techniques used acid solution to titrate vacancies in the solid base catalyst in the methanol solution. The acidic agent reacted with the basic site on the top layer and desolved it into solution. It could be suggested that the data of basic sites from the approximated titration could be the total basic sites of the bulk catalyst, with the CO_2-TPD being equal to the amount of basic on the surface. Similarly, results were also found with KNO_3/Al_2O_3 that CO_2-TPD designated the amount of basic sites exposed at the top of the overlapped structure while the titration could represent all basic sites [22].

Figure 6.6A shows that ^1H NMR of mordenite zeolite spectrum peaked at 3.62 ppm. This could be ascribed as the bridging of the hydroxyl group (SiOHAl) which formed H-bonding with the water molecules. Free protons from the water combined with oxygen on the zeolite [23]. The oxygen molecules of water absorbed physically into the cation (Na^+) which boned with oxygen on the zeolite catalyst. The FIIR result corresponds to NMR that OH broad band of isolated and bonded stretching (3650 cm^{-1} and 3000–3500 cm^{-1}) was found. It could be identified that the water molecule strongly absorbed in the zeolite framework. After loading K at 20 %wt, a peak of spectra at 1.27 and 6.29 ppm appeared. The signal at 1.2 ppm as a trace of physically absorbed water on the cation was originally observed by Vyalikh *et al.* 2007 [24]. The shifted peak from 3.6 ppm to 6.3 ppm was found due to higher size of cation. The progressively bigger cation size diffused into the pores and the sensitive physicochemical structure changed with the parent Na+ in the sodalite cage. The balancing charge, therefore, occurred on the zeolite extraframework. The K^+ cation exchanged with the Na^+ on the mordenite zeolite. The larger ionic radius was expected to occupy sites I and II in the supercage. This peak shift could also be ascribed to the electrostatic interaction bridge of the hydroxyl proton to the adjacent framework of oxygen. The chemical shift provided useful information in explaining the strong K^+ cation with the oxygen framework while also displaying increase basic strength of the catalyst. Bosch *et al.* 2001 noted that the basic strength could be estimated from the proton chemical shifts which caused increasing size of the alkali-metal cation such as exchanging K or Cs from NaY into KY or CsNaY [25].

Potassium adsorption took place on the framework, thus leading to chemical shifts. With further loading of K to 30 wt%, the chemical shift increased due to a high quadrupolar interaction of potassium.

6.4.2 Influence of Calcination Temperature

The XRD patterns of the calcined samples at 400 °C, 500 °C, and 600 °C Figure 6.1(f–h) correspond with the same XRD patterns of the uncalcined 20 wt% KOH/mordenite samples. However, when increasing the calcination temperature, the calcined catalyst became more amorphous.

The SEM results of the catalysts calcined at 400 °C to 600 °C are illustrated in Figure 6.2(g–i). The particles are agglomerated and irregular in shape, with a substantial variation in particle size. The discrepancy that we observed between the effect of calcination carried out on uncalcined and calcined catalyst, is most likely attributed to a slight decrease in crystallinity of the calcined catalyst, particularly in samples calcined at high temperature.

After calcination, there was an increase of Si/Al ratio or decrease of Al atom which resulted in decreasing anion of AlO_4^-. It could be ascribed as dealumination. Removal of the framework Al after calcinations caused morphology which increased particle size while surface area decreased. Therefore, high calcination temperature altered the Si/Al value, which changed the physical properties of the catalyst.

The effect of calcination temperature on the basic strength, given in Table 6.1, demonstrated no difference in basic strength was found between the uncalcined and calcined 20 wt%K/mordenite catalysts. However, the total basic sites of the calcined catalysts continuously decreased from 5.16 mmol/g to 2.21 mmol/g of catalyst when the calcination temperature was increased. This could be due to the collapse of the pore structure, as represented by using FE-SEM, Moreover, Zhu *et al.* (1999) proposed that the KNO_3 dispersed on zeolite has difficulty thermally decomposing even during evaporation at 600 °C, hence only a weak basic sites is produced. It could be concluded that decomposition of KOH under high temperatures on mordenite lead to a decrease in the basic sites of the catalyst [26].

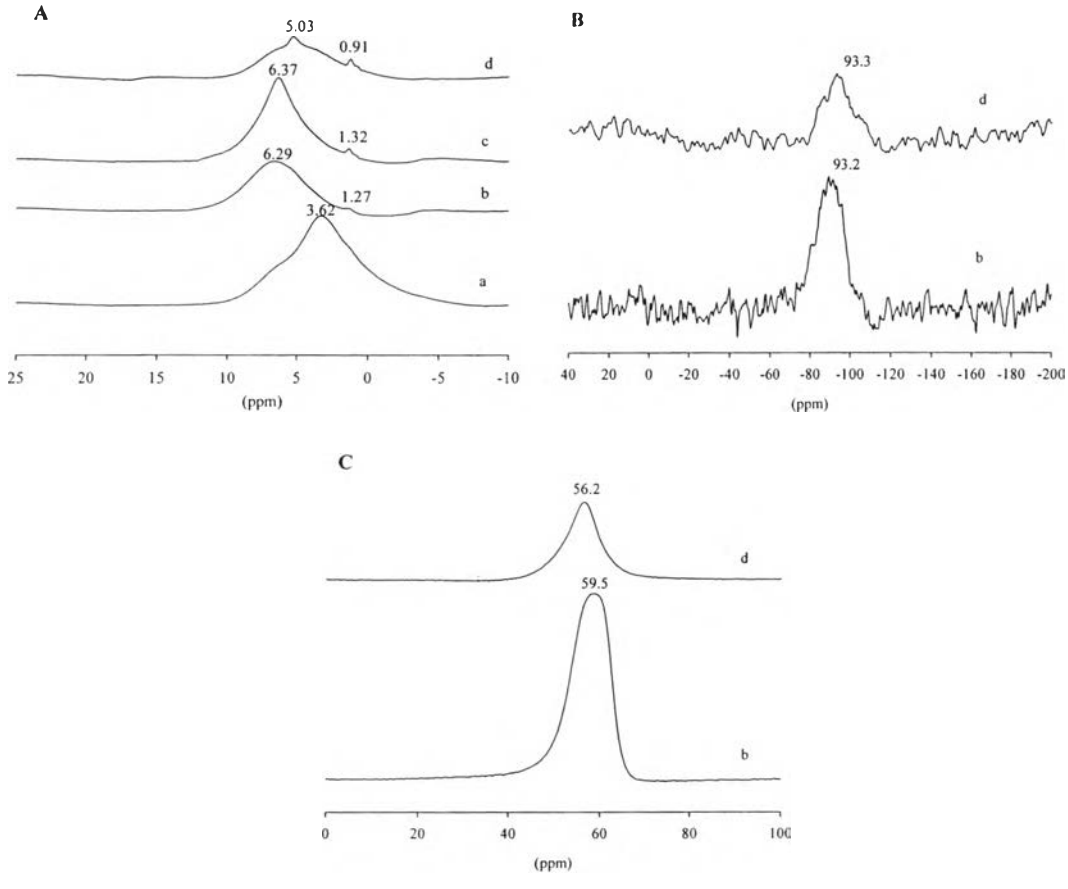

Figure 6.6 A, ^{1}H NMR spectra of uncalcined (a) mordenite, (b) 20 wt% K/mordenite, (c) 30 wt% K/mordenite, and calcined (d) 20 wt% K/mordenite: B, ^{29}Si NMR spectra of (b) uncalcined 20 wt% K/mordenite, and (d) calcined 20 wt% K/mordenite: C, ^{27}Al NMR spectra of (b) uncalcined 20 wt% K/mordenite, and (d) calcined 20 wt% K/mordenite.

The 20 wt%K on mordenite calcined at 500 ºC is shown in Figure 6.6A.d. NMR peaks appeared when the peak was shifted from 6.3 ppm to 5 ppm, implying the basic strength of the catalyst should be decreased due to lower electronic balance with the cation; however, the ^{1}H NMR is not inadequate to the understand topology and crystallographic of the calcined catalyst. Therefore, ^{29}Si and ^{27}Al were investigated, as illustrated in Figures 6B and 6C, respectively. The large broad peak at -93.3 ppm was assigned to $Si(OSi)_4$ with a shoulder peak of -85 and -110 ppm could be identified to be a dipolar magnetic interaction of protons with the

$Si(OSi)_3(OAl)$ framework [27,28]. The patterns of calcined catalyst were similar to the uncalcined catalyst, indicating that after calcinations of the catalyst the silicon structure did not change in framework unit. Figure 6.6C shows the spectrum line at 59.5 ppm referred to $Al(H_2O)_6^{3+}$ [29]. This peak was found to be tetrahedral framework aluminum. After calcination, spectrum was deducted from 59.5 ppm to 56.2 ppm which accounts for the change in the aluminum framework. The aluminum atoms were not stablilized in the framework under high calcination temperatures. By comparing the shift in ^1H NMR results of the calcined catalyst, a decreased bridging of hydroxyl, $Al\text{-}O^- H^+$; or number of electron sites; ions which are normally generated by cooperation with the aluminum atom in the framework. It may be noted that the aluminum atoms were the primary factors which were regularly involved with basic sites via the electronic charges that were introduced in the framework through the AlO_4 tetrahedral.

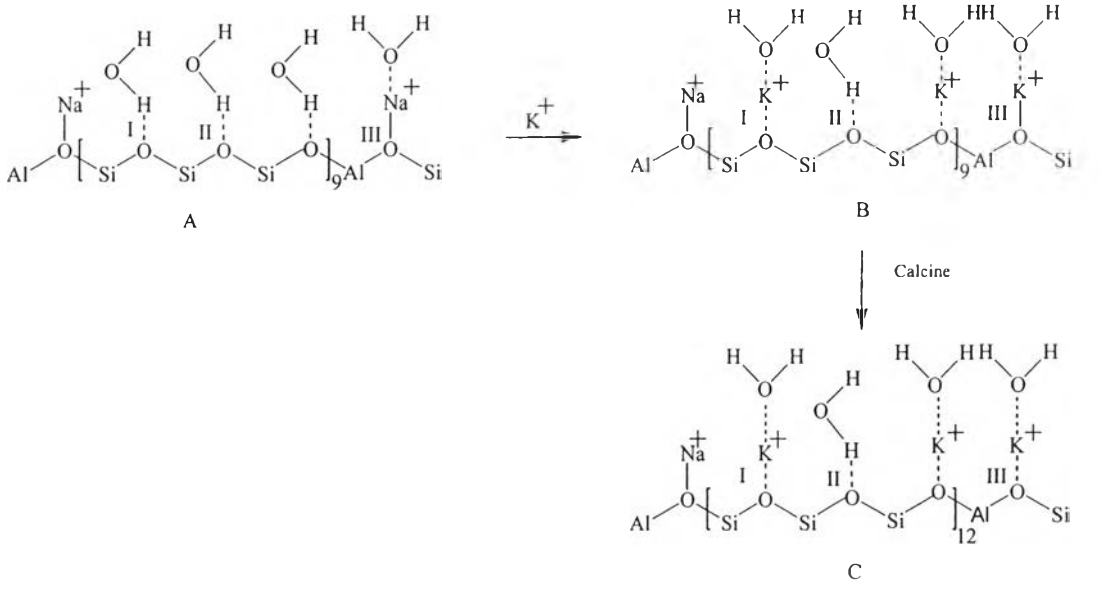

Figure 6.7 Scheme of the global basicity cluster in mordenite.

The influence of potassium hydroxide loading and calcination temperatures may affect on the basic properties of mordenite zeolite. The loading of cations (such as alkaline) adhered with a negative charge on the framework oxygen. The basic strength of zeolite depended on the Si–O–Al angle and T–O distance, and

O–M distance (where M is an exchanged alkaline cation) [30]. The larger size of exchanged potassium instead of sodium caused a greater distance which resulted in higher basic strength. Not only the size of the cation diameter, but also the high amount of potassium cations increased basic strength due to intense electropositivity of the counteraction in zeolite [31]. Thus, increased potassium loading created a rich-positively charged surface which could quickly react with the methanol to form methoxide.

Barthomeuf, (2005) proposed that the basic strength of zeolite depends on the Al location and the basic site was evaluated for the number of Al in tetrahedral framework [32]. Figure 6.7 shows the mechanism of KOH on zeolite via hydrogen bound with oxygen adjacent alumina and silicon sites and two silicon sites, respectively. Water molecule dispersion on the AI and AII sites displayed hydrogen bonding with oxygen framework. These peaks should actually reveal from 1.8 ppm to 2.2 ppm; however, with interference from the broad peak of the AIII oxygen structure of water formed with the Na^+ cation, because a strong electronic effect adhered to the positive charge of the cation. Exchange of cations was observed when loading K^+ into the framework at the BIII site, and then the immense chemical shift of hydroxyl groups of absorbed water in the zeolite catalyst was from 3.6 ppm to 6.2 ppm. In addition, some excess K^+ was absorbed with oxygen from adjacent alumina and silicon sites and two silicon sites as shown in Figure 6.7.BI. That resulted in broader peak and higher chemical shift. However, the peak at 1.3 ppm still appeared without interference of spectrum from the cation. It could be attributed to the residue of the hydrogen bond of water and vacancy site of oxygen on the mordenite surface (Figure 6.7.BII). After calcination of the catalyst at the high temperature, dealumination or decreasing of Si/Al ratio resulting in downfield shift occurred. The reduction of alumina had decreased the CIII site in zeolite which had the highest electron density. The chemical environment of AlO_4 tetrahedral was considered to be the species which create strong basic sitesby looking at the (SiO)a(AlO) sequences around any given framework aluminum taken as origin [33]. The variable a represents the number of SiO between AlO that substance for a = (1, 2, 3,...). The a =1 represents the highest basic sites due to close of Al atoms. The oxygen atoms (a >2) were less basic observe and farther from the AlO_4 tetrahedral. The dealumination

of the mordenite zeolite occurred when a, or SiO repeating unit, was increased from 9 to 12. It could be noted that strong basic sites had deducted since the CI and CII sites increased instead of the CIII site. Moreover, removal of alumina during calcinations also decreased basic site of mordenite catalyst.

6.4.3 Batch Transesterification Reaction

6.4.3.1 Influence of Reaction Time on the Methyl Ester Content

Influence of the reaction time on the methyl ester yield of KOH/mordenite catalyst was studied, as shown in Table 6.2. The results showed that at 2 h, no activity had occurred yet the highest methyl ester content was observed at 3 h and decreased slightly through the remaining 7 h of testing time. The decrease in methyl ester content and long reaction time happened when the side and reversible reactions occurred. Therefore, maximum methyl ester yield was obtained 96.67 wt% at 3 h.

6.4.3.2 Influence of Potassium Loading on the Methyl Ester Content

The dependence of potassium loading on the KOH/Mordenite catalyst was investigated. The results are illustrated in Table 6.2. At 5 wt%, the KOH/Mordenite catalyst showed no activity. The methyl ester yield was increased when the loading amount of K was increased from 10 to 20 wt%, afterward it remained constant to 25 wt% because, from the chemical characterization, the basic strength and basic sites was not raised. When the loading amount of K was increased to 30 wt%, the methyl ester content rapidly decreased. The reduction of methyl ester content was obtained with 30 wt% because the high loading amount of KOH destroyed the structure of mordenite which could be observed from the XRD and XRF. The crystal structure was dramatically collapsed and the Si/Al ratio was decreased, which revealed a change in its framework structure and its physical structure. In addition, the results illustrated the decrease of the basic site and lowering of the surface area of the catalyst were obtained by the excess KOH. The highest methyl ester yield (96.67 %) was obtained at a KOH loading of 20 wt% on mordenite.

6.4.3.3 Influence of Molar Ratio of Methanol/Oil on the Methyl Ester Content

To investigate the effect of the molar ratio of methanol/oil on the KOH/Mordenite catalyst, the experiment was carried out with various molar ratios of methanol/oil from 6:1 to 21:1. Normally, the stoichiometry of transesterification reaction requires 3 mol of methanol per mol triglyceride to yield 3 mol biodiesel and 1 mol glycerol. To accelerate biodiesel yield, an excess amount of methanol was used to shift the equilibrium of transesterification to the right-hand side.. The methyl ester yield (Table 6.2) was low at molar ratio of 6:1 due to a limiting of mass transfer between the surface of the oil and methanol and active sites that it would be caused to low amount of methoxide as an intermediate. When increasing the molar ratio of methanol/oil from 6:1 to 12:1, the methyl ester yield increased considerably. Beyond the molar ratio of 15:1, the excess methanol had no significant effect on the methyl ester content. When the amount of methanol was over 18:1, glycerol separation became more difficult, thus decreasing the biodiesel yield. This phenomenon has also been found by other researchers [34]. The maximum methyl ester content of 96.67 wt% was obtained when the molar ratio was 15:1.

6.4.3.4 Influence of Amount of Catalyst on the Methyl Ester Content

To study the effect of the amount of KOH/Mordenite catalyst, the amount of catalyst was varied from 1 to 6 wt%. The results shown in Table 6.2 indicated that the methyl ester content increased when the catalyst amount was raised from 1 to 3 wt%. But further increasing of the catalyst amount, the methyl ester yield was decreased because a mixing problem of reactant, catalyst, and product. The products became too viscous and required demand of high power consumption for adequate stirring. The maximum methyl ester yield of 96.67 wt% was obtained at 3 wt% of catalyst.

6.4.3.5 Influence of Calcination Temperature on the Methyl Ester Content

The influence of calcination temperature on the methyl ester content was investigated within the range of 400 °C to 600 °C. Table 6.2 illustrates when increasing the calcination temperature, the methyl ester content decreased. The

decreased in catalytic activity at high temperatures occurred because of the loss of potassium species by evaporation or sublimation. The XRD and XRF results indicated that the structure of mordenite changed in term of chemical composition, which corresponded the chemical results of the Hammett indicator and acid titration; the basic site of calcine catalyst decreased with increasing calcination temperature. Moreover, there was collapse of porosity in the zeolite which lead to decreased surface area and reduced catalytic activity observed by the N_2 adsorption-desorption and the SEM. Thus the uncalcined catalyst had a methyl ester content of 96.67 wt%, which exhibited higher activity than that of the calcined KOH/Mordenite catalyst.

6.4.4 Packed-bed Transesterification Reaction

6.4.4.1 Influence of Reaction Time on the Methyl Ester Content

The influence of reaction time on the methyl ester yield was varied from 0 to 8 h at conditions of 20 %K/mordenite, methanol/oil molar ratio 15:1, flow rate 11 ml/min, reaction temperature of 60°C, and 12 wt% amount of catalyst. The methyl ester content increased between 2 and 4 h to over 90 wt%, thereafter it remained steady, and the amount decreased between 6 and 8 h. The maximum methyl ester content of 94.54 wt% was achieved at 4 h reaction time.

6.4.4.2 Influence of Catalyst Particle Size on the Methyl Ester Content

The effect of the catalyst particle size of the 20 %K/mordenite on the methyl ester yield was also investigated by varying the mesh size from >20 to 40–50 mesh. It was observed that the methyl ester content decreased with the larger catalyst particle size. The maximum methyl ester content of 94.54 wt% was obtained with the mesh size of 40–50 mesh, which was the smallest size.

Table 6.2 Effect of process variable on transesterification of palm oil in batch reactor

Time (h)	KOH loading (%wt)	MeOH/Oil Molar ratio	Amount of catalyst (%wt)	Calcination Temperature (°C)	Methyl ester yield (%wt)
2	20	15:1	3	-	0
3	20	15:1	3	-	96.67
4	20	15:1	3	-	94.26
5	20	15:1	3	-	95.18
6	20	15:1	3	-	93.64
7	20	15:1	3	-	90.22
3	5	15:1	3	-	0
3	10	15:1	3	-	89.01
3	15	15:1	3	-	92.84
3	20	15:1	3	-	96.67
3	25	15:1	3	-	96.81
3	30	15:1	3	-	70.11
3	20	6:1	3	-	70.98
3	20	9:1	3	-	86.63
3	20	12:1	3	-	91.57
3	20	15:1	3	-	96.67
3	20	18:1	3	-	93.73
3	20	21:1	3	-	95.67
3	20	15:1	1	-	88.57
3	20	15:1	2	-	93.34
3	20	15:1	3	-	96.67
3	20	15:1	4	-	92.25
3	20	15:1	5	-	93.24
3	20	15:1	6	-	88.57
3	20	15:1	3	400	82.64
3	20	15:1	3	500	38.12
3	20	15:1	3	600	18.12

6.4.5 Comparisons between Batch and Packed-bed Reactors

The comparison between the two different types of reactor for biodiesel production using 20 %K/mordenite as solid catalysts is shown in Table 6.1. The batch experiment took a shorter reaction time to obtain higher methyl ester content than the packed-bed reactor. The packed-bed system experiment, the reactant and methanol passed through the packed catalyst over a period of time. The contact time of the reactant and catalyst was rather short, leading to a longer reaction time. In the point of catalyst size, the optimum catalyst particle size of the batch reactor was 10–20 mesh. However, 40–50 mesh was the optimum catalyst particle size on the

packed-bed reactor. It could be deduced that the small particle size was more suitable for the packed-bed reactor because the higher surface area of catalyst increased the more contact area between reactant and catalyst, leading to a higher percentage of product.

6.4.6 Recycling of the Catalyst

After the selection of the best catalysts, the influence of the reaction parameters on activity of the catalyst was studied in detail. The used catalysts were recovered by simple filtration and remaining amounts of catalyst were used to catalyze in the next cycle batch. Table 6.1 displays the methyl ester content and the run number of the 20 wt% K/mordenite. A remarkable reduction in catalytic performance was observed, yielding 72.33 wt% and 40.24 wt% of methyl ester contents in the second and third runs for KOH/mordenite catalyst, respectively. The potassium leaching of KOH/mordenite in the mixtures was 0.096 and 0.076 wt% of KOH in palm oil in the first and second runs, respectively, suggesting that the active species were somewhat leached from the solid support.

Moreover, the different types of reactor were used to investigate the reuse runs. The recycle catalyst was tested in the packed-bed reactor with an optimum reaction parameter. For packed-bed reactor, the calculated potassium leaching of KOH/mordenite in the mixture of 0.086 wt% of palm oil is shown in Table 6.1. The amount of the potassium leaching from packed-bed reactor was lower than that of potassium leaching from batch reactor. It should be noted that the agitation of the stirrer in the batch increased the rate of potassium leaching because it changed the molecular structure of catalyst from larger to smaller sizes and removed some physisorption of potassium on the surface—lacking of chemical stability—in the mixture due to the interaction between the alcohol (polar solvent) and active sites of catalyst. Thus, the packed-bed reactor was able to retain the active species during the run. The advantages of a packed-bed reactor for reuse and regeneration may become an attractive because of the possibility of longer operation times and no filtration would be required in the process.

To clarify the decline of activity in successive runs, the basic strength of used catalyst was the same as the fresh catalyst as shown in Table 6.1. It was

noted that the basic site of used catalyst was lower than that of the fresh one approximately a quarter in first and second runs. It seems that the amount of basic strength should be enough to promote activity for transesterification in recycle runs, whereas, the activity of spent catalyst declined with successive runs.

In order to attain less leaching of potassium, the decrease of activity could come from a cover of reacted mixture—intermediate mono- and di-glyceride, biodiesel, and glycerol—and excess methanol. Firstly, the excess methanol was removed by evaporating it at 110 °C for 24 h before use in the reaction. The surface area of the spent catalyst, shown in Table 6.1, shows that the spent 20 wt% K/mordenite in first and second run was lower than the fresh catalyst. The pore volume of the spent catalyst disappeared due to coverage of mixture of species inside pore. The result of FTIR (Figure 6.4c) revealed that the peak of spent catalysts also demonstrated new absorption peaks as a result of the oil deposition during the reaction. The new peaks were found at 2922 cm^{-1}, 1740 cm^{-1}, and 1160 cm^{-1}, which were credited to the C–H, aldehyde (C=O), and ester (C–O), respectively [35–37]. Other new peaks were observed at 1465 cm^{-1} and 1375 cm^{-1}, which could be attributed to the bending absorption of the methylene (CH_2) and methyl (CH_3) groups. Moreover, the spent catalysts had a higher intensity of broad band peak at 3300 cm^{-1} – 3700 cm^{-1}, which corresponded to the O–H band of the physically absorbed water on the molecule. Nevertheless, the peaks of mordenite support still appeared on the spent catalysts spectra.

The spent 20%K/mordenite catalyst was washed by commercial grade acetone. The acetone was pumped at flow rate of 11ml/min into reactor, which was packed by the spent catalyst, and left it for 1 h. Next, spent catalyst was evaporated in an oven at 110 °C for 24 h. The FTIR spectrum of treated K/mordenite is shown in Figure 6.4d. It was clearly observed that the absorption peak at 3450 cm^{-1} decreased in relation to the removal of oil from the surface of catalyst. In addition, the spectrum of the treated catalyst was similar to that of the fresh catalyst. It could be inferred that after treating with acetone, the spent catalyst could be recovered the same as the fresh catalyst.

Figure 6.2 shows the SEM micrographs of the fresh, spent, and treated K/mordenite catalysts. There was no apparent distinction between particle

size and morphology of the catalysts. On the other hand, the surface structure of the spent catalyst was transformed once the oil was deposited on the surface. The surface structure of the treated catalyst became similar to the fresh one, implying that the property of spent catalyst should be revived. Moreover, the XRD patterns of the fresh, spent and treated K/mordenite catalysts illustrated identical diffraction peaks. There were no crystallinity or diffraction lines, implying the amorphous structure was obtained. After modification of the mordenite zeolite structure by loading with high content of KOH, the structures were transformed from a crystal phase to an amorphous phase. Deposition of the reacted mixtures and treatment of the solvent did not destroy KOH/mordenite catalyst. However, the results from EDS indicated that there was a reduction of potassium content in the KOH/mordenite catalysts due to the coverage of oil. These results agreed with the FTIR, SEM, N_2 adsorption-desorption, and XRD results. In addition, the potassium content was raised by washing the treated catalyst with acetone. The disappearance of oil agglomeration led to an increase in surface area.

The methyl ester content of the catalyst treated with acetone was analyzed by GC. A significant decrease in catalytic activity still occurred. This result was similar to the three-cycle reaction of the catalyst without pretreatment. It could be inferred that treating with acetone should not be used to improve the catalytic activity. However, this needs to be further investigated for biodiesel production.

6.5 Conclusions

Loading KOH on mordenite is a strongly efficient catalyst for transesterification of palm oil with methanol. The highest activity of methyl ester yield was obtained of 96.67 wt% with potassium loading of 20 wt% in a batch reactor; optimal reaction time of 3 h, catalyst at 4 wt%, and a methanol-to-oil molar ratio of 15:1. The 20 wt%K/mordenite gave high basic strength and the highest basicity. When loading KOH over 25 wt%, the excessive amount of potassium hydroxide had an ability to decrease crystallinity and surface area. However, the calcined 20 wt%K/mordenite was found to show lower activity than uncalcined catalyst at the optimum conditions as mentioned above. At high temperature

pretreatment, the collapsed pore structure of the mordenite and dealumination occurred. In addition the basic sites also decreased with increasing calcination temperatures.

The comparative study of the different reactors, batch and packed-bed reactor, for biodiesel production using a 20 wt%K/mordenite catalyst has demonstrated that the packed-bed reactor exhibited similar catalytic activity to the batch reactor. The leaching of K species measured by XRF showed a relatively low amount of K leaching from the solid support during the reaction. The packed-bed reactor prompted the heterogeneous catalyst to tolerate a higher level of leaching than the batch reactor.

6.6 Acknowledgements

This work was supported financially by the National Metal and Materials Technology Center, Thailand, and the Center of Excellence on Petrochemicals and Materials Technology, Thailand.

6.7 References

[1] J.V. Gerpen, Fuel Process. Tech. 86 (2005) 1097–1104.

[2] J. Hu, Z. Du, C. Li, E. Min, Fuel 84 (2005) 1601–1606.

[3] S. Pehan, M.S. Jerman, M. Kegl, B. Kegl, Fuel 88 (2009) 970–979.

[4] S.M.P. Meneghetti, M.R. Meneghetti, C.R. Wolf, E.C. Silva, G.E.S. Lima, L.L. Silva, T.M. Serra, F. Cauduro, L.G. Oliveira. Energ. Fuel 20 (2006) 2262–2265.

[5] I. Lukić, J. Krstić, D. Jovanović, D. Skala, Bioresour. Technol. 100 (2009) 4690–4696.

[6] X. Bo, X. Guomin, C. Lingfeng, W. Ruiping, G. Lijing, Energ. Fuel 21 (2007) 3109–3112.

[7] W. Xie, H. Li, J. Mol. Catal. A-Chem. 255 (2006) 1–9.

[8] D.M. Alonso, R. Mariscal, R. Moreno-Tost, M.D.Z. Poves, M.L. Granados, Catal. Commun. 8 (2007) 2074–2080.

[9] K. Noiroj, P. Intarapong, A. Luengnaruemitchai, S. Jai-In, Renew. Energy 34 (2009) 1145–1150.

[10] M.J. Ramos, A. Casas, L. Rodríguez, R. Romero, A. Pérez, Appl. Catal. A: Gen. 346 (2008) 79–85.

[11] G.J. Suppes, M.A. Dasari, E.J. Doskocil, P.J. Mankidy, M.J. Goff, Appl. Catal. A: Gen. 257 (2004) 213–223.

[12] M. Bender, Bioresour. Technol. 70 (1999) 81–87.

[13] J. Ni, F.C. Meunier, Appl. Catal. A: Gen. 333 (2007) 122–130.

[14] M.D. Macedonia, D.D. Moore, E.J. Maginn, Langmuir 16 (2000) 3823–3834.

[15] M. Guisnet, Q.L. Wang, G. Giannetto, Catal. Letters 4 (1990) 299–302.

[16] N. Viswanadham, M. Kumar, Micropor. Mesopor. Mat. 92 (2006) 31–37.

[17] O. Korkuna, R. Leboda, J. Skubiszewska-Zięba, T. Vrublevs'ka, V.M. Gun'ko, J. Ryczkowski, Micropor. Mesopor. Mat. 87 (2006) 243–254.

[18] S.I. Cabau, Ph.D. Thesis, Universitat Rovira I Virgili, Catalonia, Spain 2005.

[19] M. Ostroumov, P. Corona-Chávez, J. Geol. Sci. 20 (2003) 133–138.

[20] M. Di Serio, M. Ledda, M. Cozzolino, G. Minutillo, R. Tesser, E. Santacesaria, Ind. Eng. Chem. Res. 45 (2006) 3009–3014.

[21] M. Doyama, J. Kihara, M. Tanaka, R. Yamamoto, Computer aided innovation of new materials II, Elsevier, Amsterdam, 1993.

[22] Y. Wang, W.Y. Huang. Y. Chun, J.R. Xia, J.H. Zhu, Chem. Mater. 13 (2001) 670–677.

[23] L. Bertsch, H.W. Habgood, J. Phys. Chem. 67 (1963) 1621–1628.

[24] A. Vyalikh, T. Emmler, B. Grünberg, Y. Xu, I. Shenderovich, G.H. Findenegg, H.H. Limbach, G. Buntkowsky, Z. Phys. Chem. 221 (2007) 155–168.

[25] E. Bosch, S. Huber, J. Weitkampb, H. Knozinger, Phys. Chem. Chem. Phys. 1 (1999) 579–584.

[26] J. Zhu, Y. Chun, Y, Wang, Q. Xu, Catal. Today 51 (1999) 103–111.

[27] T. Beutel, M.J. Peltre, B.L. Su, Colloids Surf. A: Physicochem. Eng. Aspects 319 (2001) 187–188.

[28] S.A. Axont, J. Klinowski, J. Phys. Chem. 98 (1994) 1929–1932.

[29] B.H. Wouters, T.H. Chen, P.J. Grobet, J. Am. Chem. Soc. 120 (1998) 11419–11425.

[30] A, Auroux, Mol. Sieves 6 (2008) 45–152.

[31] M. Huang, S. Kaliaguine, M. Muscas, A. Auroux, J. Catal. 157 (1995) 266–269.

[32] D. Barthomeuf, J. Phys. Chem. B 109 (2005) 2047–2054.

[33] D. Barthomeuf, Micropor. Mesopor. Mat. 66 (2003) 1–14.

[34] H. Liu, D. Chaudhary, S.I. Yusa, M.O. Tadé. Carbohydr. Polym. 83 (2011) 1591–1597.

[35] X. Liu, H. He, Y. Wang, S. Zhu, Catal. Commun. 8 (2007) 1107–1111.

[36] S.J. Oliveira, R. Montalvão, L. Daher, P.A.Z. Suarez, J.C. Rubim, Talanta 69 (2006) 1278–1284.

[37] M.F. Ferrão, M.S. Viera, R.E.P. Pazos, D. Fachini, A.E. Gerbase, L. Marder, Fuel 90 (2011) 701–706.